Sensorless Direct Torque Control of an Induction Motor Using Fuzzy Controller

التحكم المباشر فى العزم لمحرك تأثيرى باستخدام متحكم غيمى بدون وسيلة قياس

A. A. Khalil
akhalil@aast.edu
Arab academy for science & Technology & Maritime Transport

الخلاصه : مؤخرا تعتبر المحركات التأثيرية وبخاصة القفص السنجابى هى الأوسع إنتشارا فى التطبيقات الصناعية المتغيرة السرعة، والتى تتطلب درجة عالية من الدقة والإستجابة فى السرعة والعزم لذلك توالت الكثير من الدراسات لإيجاد حلول مختلفة لرفع كفاءة أداء هذا النوع من المحركات، والتى كان من أحدثها التحكم المباشر فى العزم. ولكن نظرا لأن الطريقة التقليدية لهذا النوع من التحكم لا تأخذ فى إعتبار الإشارة الدالة على الفرق بين العزم المطلوب والمقاس أو المجال المطلوب والمقاس إذا كانت صغيرة نسبيا أو كبيرة بعض الشىء ، مما أدى إلى بطء فى إستجابة النظام خاصة فى لحظة بدء التشغيل أو أثناء مراحل التغيير فى مستوى العزم المطلوب أو المجال. من هذا المنطلق نشأت محاولة إقتراح لتقديم خطة جديدة لتحسين إستجابة ما يسمى بالتحكم المباشر فى العزم وذلك باستخدام المنطق الغيمى. لذلك الغرض ، يهدف البحث لتحقيق التحكم المباشر فى العزم باستخدام كلا من الطريقة التقليدية فى التحكم والطريقة المقترحة باستخدام المنطق الغيمى.
أهداف البحث يمكن أن تتلخص فى النقاط التالية : تصميم إستراتيجية حديثة فى التحكم على المحركات التأثيرية " التحكم المباشر فى العزم" وتقديم وإقتراح خطة جديدة فى التحكم المباشر فى العزم باستخدام المنطق الغيمى والإثبات بالإختبار والمقارنة بين نتائج كلا النظامين بتفوق كفاءة وإستجابة المتحكم الغيمى على المتحكم التقليدى.

Abstract: In this paper direct torque control DTC of an induction motor is developed. A new technique for DTC based ou fuzzy logic concept is proposed, where fast torque response with low ripple in the stator flux and torque of induction motor can be achieved. In comparison with the conventional DTC simulation results clearly demonstrate a better dynamic and steady state performance with the fuzzy logic DTC. The two approaches are explained in clear details , which are designed using SIMULINK under Matlab Ver.6 software package. Also, MATLAB/FUZZY toolbox is used to implement the fuzzy logic controller. Both systems are simulated under the same conditions.

I. Introduction

variable speed AC motor drives have been continuously developed during the last decades owing to the advances in power electronics, control theory and microprocessors technology. In recent industrial development, induction motor is widely used for variable speed control system, which requires a precise and quick torque response. An improvement of the drive performance can be obtained using a new direct torque control algorithm based on the application of the space vector modulation [1-3]. The Direct Torque Control (DTC) technique has been recognized as viable method to provide a very quick and precise response, where minimum switching frequency and hence maximum efficiency is guaranteed and fully de-coupled control loops as well. Direct torque control is one of the actively researched control schemes which are based on the de-coupled control of flux and torque when the exact vector of stator flux is known. The basic concept of direct torque control of induction machines is investigated in order to emphasize the effects produced by a given voltage vector on stator flux and torque variations. In DTC, the torque and stator flux are regulated to their command values by selecting the switching state which gives the proper changes in the torque and flux. There have been some DTC-based strategies, e.g. voltage-vector selection using switching table, direct self-control, and space-vector modulation [4 - 6]. Among them, the voltage-vector selection strategy using a switching table is widely researched and commercialized, because it is very simple in concept and easy to be implemented. The proper voltage vector selection is based on the error in electromagnetic torque, error in stator flux and the position of the stator flux vector. In the conventional DTC scheme the system makes no difference between a very small and relatively large error of torque and/or flux. The switching states chosen for the large error that occurs during the startup or during a step change in torque command or even flux command are the same that have been chosen for the fine control during normal operation. This may cause a lightly slower response during the start-up and during a step change in electric torque or stator flux. This was the reason of attempting to propose a new approach for direct torque control (DTC) based on "If the range in which the torque error exists and the range in which the flux error exists are considered when choosing the switching state, the system response can be improved using different error levels". A type of controller that allows the control rules to be adjusted according to the value of the inputs is a fuzzy logic controller. Fuzzy logic controller is one of the more efficient AI (Artificial intelligence) techniques used in control applications because it is a controller that converts a set of linguistic rules based on expert knowledge into an automatic control strategy [7-14]. So, fuzzy logic control is used for the implementation of direct torque control of an induction motor in a way of trying to improve its slow response.

II. Strategy of Direct Torque Control

The basic concept of DTC is to control the stator flux and torque directly by using the effective voltage vector generated from voltage source 6-step inverter. This method was offered by Takahashi in 1985 [15]. The idea is that motor flux and torque are used as primary control variables, which is contrary to the way in which the traditional AC drives control input frequency and voltage. In DTC algorithm, a direct hysteresis stator flux and electromagnetic torque control that trigger directly one voltage vector among the six effective voltage vectors (V_1, V_2, V_3, V_4, V_5, V_6), and two null voltage vectors (V_0, V_7), in order to keep stator flux and torque within pre-specified error tolerance bands as shown in figure (1).

Accepted February 15, 2003.

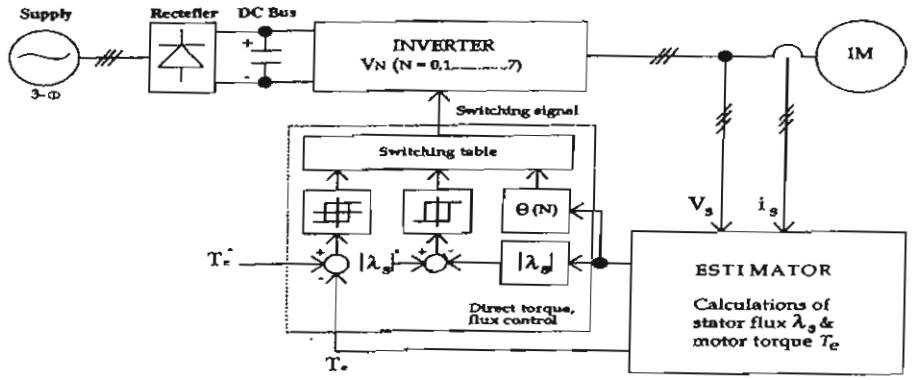

Figure (1) Direct torque and flux control scheme.

The proper selection of the inverter switches forces the stator flux vector in the direction where the reference values of the motor torque and the stator flux are achieved. Motor model estimates the actual torque, stator flux, and stator flux vector position by means of measurements the motor phase currents and voltages. The optimum selection of the inverter switching modes, both errors of the flux and torque shall be within the hysteresis bands as shown in figure(2) and figure(3) and inquest the fastest torque response and the highest efficiency at every instant. This can be achieved by evaluation of actual flux, actual torque and the position of the stator flux vector.

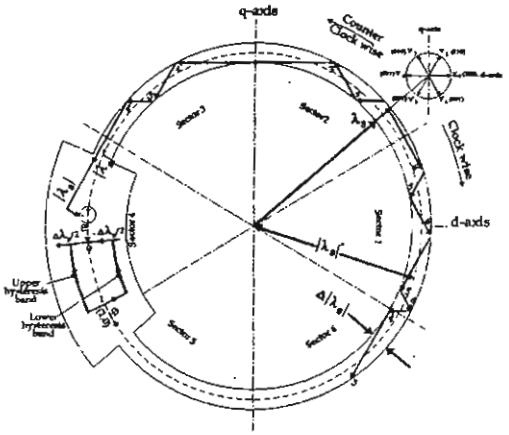

Figure (2) Trajectory of the stator flux space phasor with two-level hysteresis controller.

The proper selection of the inverter switching states is made so that the error between estimated stator flux and the stator flux command signal must be within the pre-specified hysteresis band, where

$$|\lambda_s|^* - \Delta|\lambda_s|/2 \le |\lambda_s| \le |\lambda_s|^* + \Delta|\lambda_s|/2 \qquad (1)$$

The selection of the inverter switching states depends not only on the error of the flux amplitude but also on the direction of stator flux. The stator flux vector position is determined by equation (2)

$$(2N-3)\pi/6 \le \theta(N) \le (2N-1)\pi/6 \qquad N = 1,2,...6 \qquad (2)$$

For example, if (λ_s) is in the region of sector (2), as shown in figure (2). For clockwise direction of rotation, when $|\lambda_s|$ reaches the upper limit of equation (1), the voltage vector V_6 must be selected. When $|\lambda_s|$ reaches the lower

limit of equation (1), V_1 must be selected. On the other hand, for counterclockwise direction of rotation, when $|\lambda_s|$ reaches the upper limit for the same sector, V_4 must be selected. When $|\lambda_s|$ reaches the lower limit of equation(1), V_3 must be selected. Thus, two dimensional hysteresis control of (λ_s) makes possible of a constant $|\lambda_s|$ by selecting the appropriate voltage vectors.

As a result, the flux vector can be freely driven in steps through a hysteresis controller, so that the error between (T_e) and (T_e*) must be within a pre-specified hysteresis band ($|\Delta T_e|$) which is presented as:

$$T_e^* - \Delta T_e \le T_e \le T_e^* \quad \text{(when } (\lambda_s) \text{ rotates in the forward direction)} \qquad (3)$$

$$T_e^* \le T_e \le T_e^* + \Delta T_e \quad \text{(when } (\lambda_s) \text{ rotates in the backward direction).}$$

As shown in figure(3), for motoring case (i.e. the flux space phasor rotates in counterclockwise direction), when (T_e) reaches ($T_e^* - \Delta T_e$), one of the accelerating voltage vectors must be applied on the motor terminals to reduce the error between (T_e) and (T_e^*) to be within (ΔT_e). Likewise, in the case of braking or reverse operation (i.e. the flux space phasor rotates in clockwise direction), when (T_e) reaches ($T_e^* + \Delta T_e$), one of the decelerating voltage vectors must be applied to reduce the error to be within ($-\Delta T_e$). With the proper selection of optimum voltage vectors would be realized by taking into consideration equation (1), to maintain (λ_S) within acceptable limits. Accordingly the constant torque control could be achieved. In general, the explanation of DTC strategy is that, the error of stator flux magnitude and the error of electromagnetic torque can be detected and digitized, respectively by simple two-level hysteresis comparator, three-level hysteresis comparators, and the stator flux vector location passing through

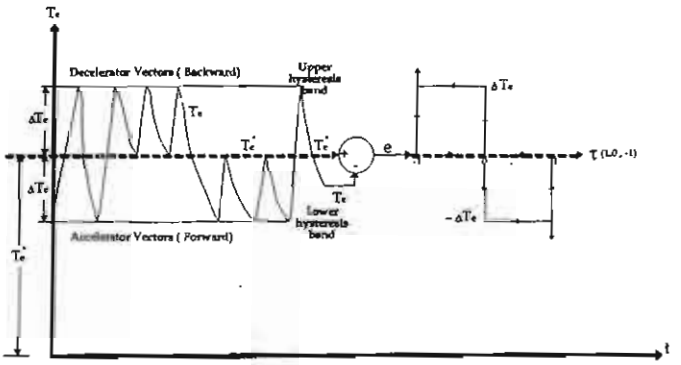

Figure(3) Representation of torque control using three-level hysteresis controller.

the six 60°-sectors, which can be obtained according to table (1).

Table (1) Sign detectors (Simple comparators).

Sector / Sign detector	1	2	3	4	5	6
$Sign\ (\lambda_{ds})$	+	+	-	-	-	+
$Sign\ (\lambda_{qs})$		+	+		-	-
$Sign\ (\sqrt{3}\lambda_{ds} - \lambda_{qs})$	-	+	+	-	+	+
$\Theta_s(N)$	$\Theta_s(1)$	$\Theta_s(2)$	$\Theta_s(3)$	$\Theta_s(4)$	$\Theta_s(5)$	$\Theta_s(6)$

Through the two error signals and the stator flux position a proper selection of the voltage vectors can be obtained. The optimum switching states of the inverter (S_1, S_2, S_3) can be tabled versus the outputs of the comparators and the six 60°-sectors, as shown in figure (4) in which (ϕ) and (τ) signals are digitalized outputs of the comparators. and the signal of $\theta(N)$ determines an indication of the stator flux vector location [1], [5], [15].

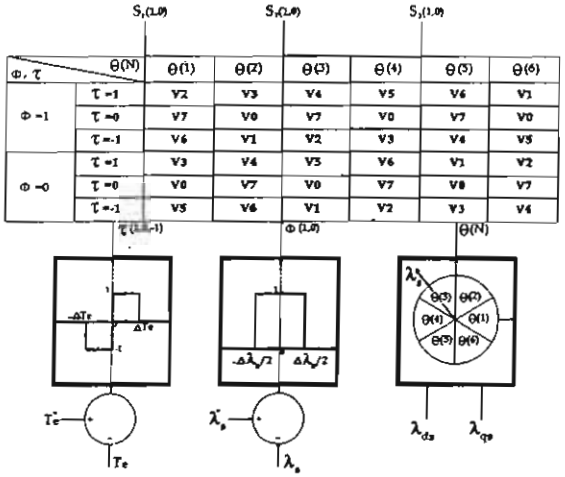

Figure (4) Selection of optimum voltage vectors referred by the outputs of the comparators along the six 60° – sectors

Where;

$\phi = 1 \Rightarrow$ for positive error of the flux magnitude. $\phi = 0 \Rightarrow$ for negative error of the flux magnitude.

$\tau = 1 \Rightarrow$ for positive error of the torque magnitude. $\tau = 0 \Rightarrow$ for torque error within the acceptable limits.

$\tau = -1 \Rightarrow$ for negative error of the torque magnitude.

III. Direct Torque Control Model

A schematic diagram of an induction motor drive under DTC is shown in Figure (5). The induction motor is fed

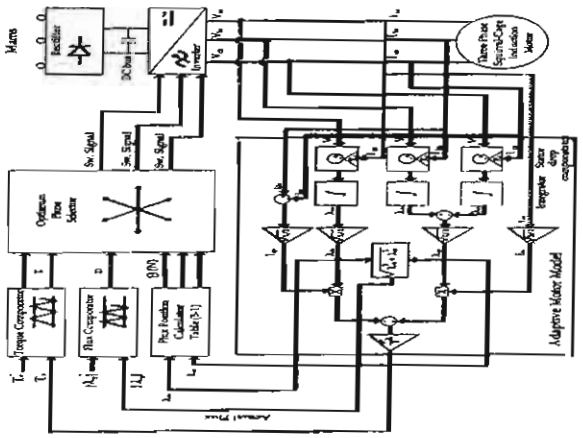

Figure (5) Complete illustrative diagram of an induction motor drive under direct torque control scheme (DTC).

from a three-phase inverter consisting of six fast switching devices, driven by control signals of optimum pulse selector. The dc input voltage is provided by a full bridge rectifier and LC filter. The stator flux and motor torque can easily be calculated using stator phase voltages and currents. The basic control algorithm of DTC is carried out

using two comparators to produce the error signals of stator flux and electromagnetic torque based on the comparison between the calculated values and their references. After digitalizing the error signals of the flux amplitude and motor torque, the output values of the hysteresis comparators provide flux and torque signals ϕ and τ respectively; representing ϕ using one bit, and τ using two bits. Where $\phi=1$ for positive error and $\phi=0$ for negative error of the stator flux magnitude, also, $\tau=(0,0)$ for torque error within the acceptable limits, $\tau=(0,1)$ and (1,0) for torque error above and below the acceptable limits, respectively. The flux vector position $\theta(N)$ is detected by three output bits. These six bits are used to access the optimum pulse selector truth table. The outputs from the truth table are used to drive the inverter switches, and the optimum voltage vector can directly be obtained.

IV. Simulation Results of Conventional DTC

Simulation was performed in order to simulate the direct torque control using SIMULINK under MATLAB Ver.6 [16]. Matlab/Simulink was used to construct the induction motor model and the strategy of DTC system. Figure (6) shows the simulation block diagram of the direct torque control of an induction motor drive system.

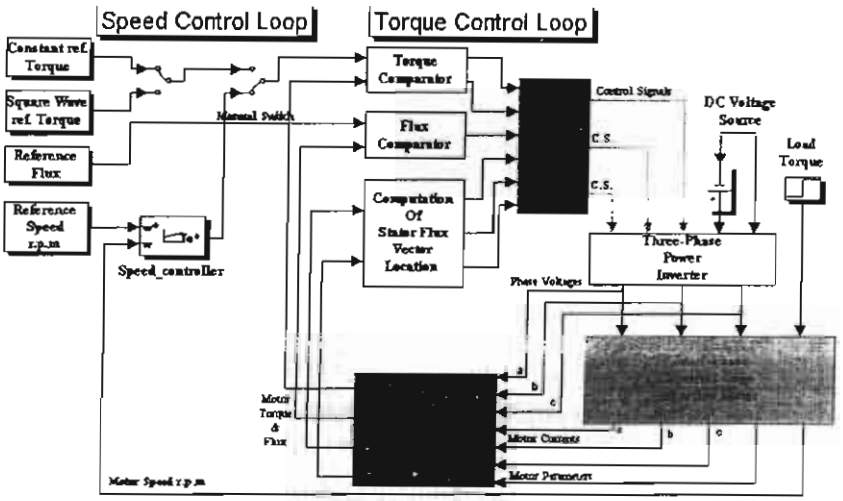

Figure (6) MATLAB/SIMULINK block diagram of the conventional DTC.

In figure (6), the reference value of the torque controller is generated by three individual input sources, as:

1. Step-input reference torque. 2. Square wave reference torque.3. Speed feedback loop using a PI controller.

Therefore, the system simulation was carried out using the above three input reference torque signals. The parameters of the selected induction motor, referred to ABB Technical Data Sheet are shown in table (2) given in the appendix.

1. DTC with a Step-Input Reference Torque

The hysteresis bands for stator flux and torque controllers are set as $\lambda_{band}=0.01Wb$. and $T_{band}=1N.m$. respectively. The system was initially commanded by the rated stator flux as a constant reference value $|\lambda_s|^*=1Wb$ at $t=0$sec., while the reference torque command signal was zero ($T_e^*=0N.m.$). At $t=0.01$sec., a step change from zero to the rated motor torque $T_e^*=100N.m.$ was applied as a constant torque command signal, while the motor has been loaded by $T_L=90N.m.$ at $t=0.1$sec. The simulation results of the stator flux and motor torque are shown in figure(7). Figure(8) shows the trajectory of the d-q axis stator flux.

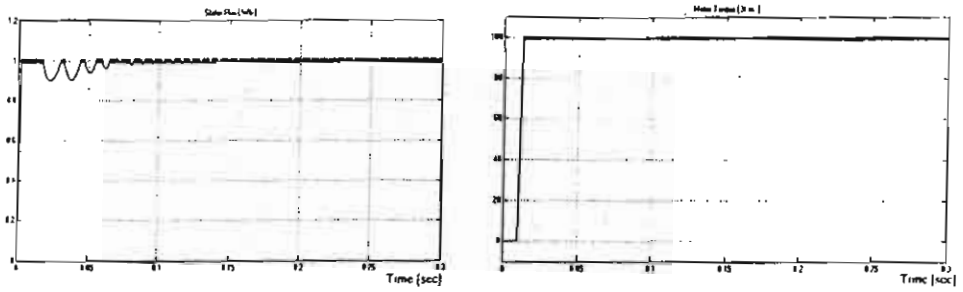

(a) (b)

Figure (7) (a) Stator flux (λ_s) (b) Motor torque (T_e)

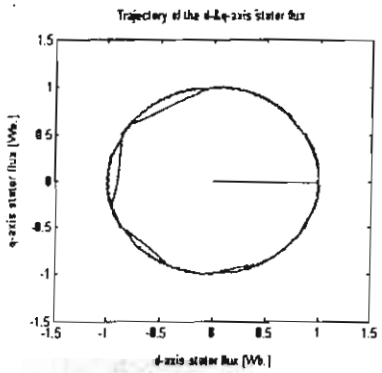

Figure (8) Stator flux space phasor during simulation

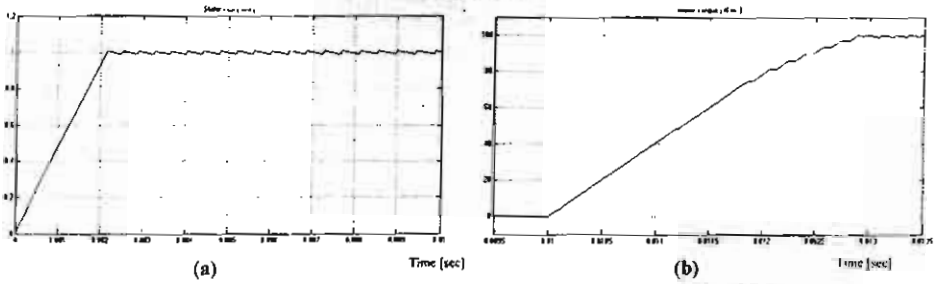

(a) (b)

Figure (9) (a) Stator flux response at starting (b) Motor torque response at starting

2. DTC with a Square Wave Reference Torque

At $t = 0.01$sec. up to $t = 0.1$sec., a step change from zero to the rated motor torque $T_e^* = 100N.m.$ was applied as a constant torque command signal. At $t = 0.1$sec. a step change in torque command signal was applied to force it to be zero $T_e^* = 0N.m.$, and this sequence is repeated. The simulation results of the stator flux and motor torque are shown in fignre(10). Figure(11) shows the trajectory of the d-q axis stator flux.

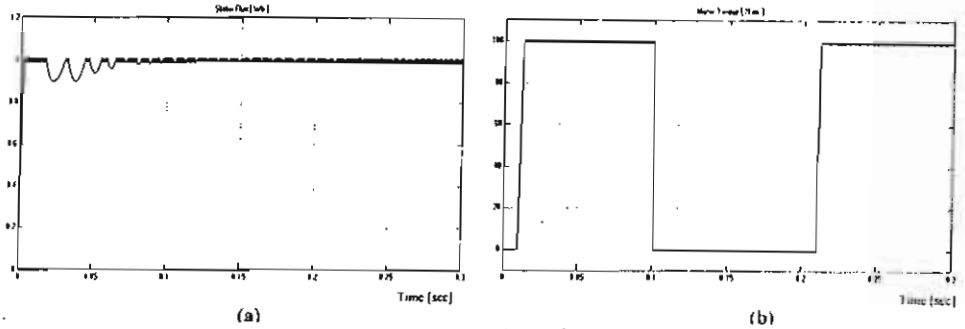

(a) (b)

Figure (10) (a) Stator flux (λ_s) (b) Motor torque (T_e)

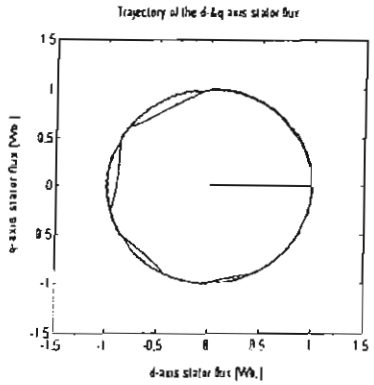

Figure (11) Stator Flux Space Phasor during simulation.

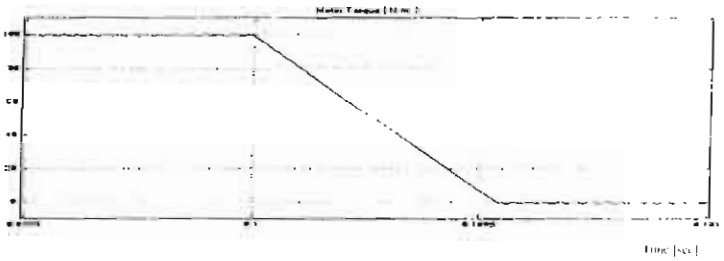

Figure (12) Electromagnetic torque response at step change in torque command singnal

Figure (12) shows the electromagnetic torque response for a step change in torque command signal (step down).

3. DTC with Speed Feedback Loop Using PI Controller

The speed control system consisting of a PI (proportional-Integral) controller technique is used to get greater speed accuracy. The external speed reference signal is compared with the actual speed produced from the motor model. The error signal is then fed to the PI controller. Thereafter, the PI controller output signal is then used as a reference input signal to the torque comparator. The PI controller gain values obtained after controller tuning as: K_p = 0.078 and K_i = 0.98. The system was initially commanded by the rated stator flux as a constant reference value $|\lambda_s|^*$ Wb at t 0 sec., while the reference command of the speed controller was zero (N_r^* 0r p.u.)

At $t = 0.01\text{sec.}$, a step change from zero speed to motor rated speed $N_r^* = 1200 r.p.m.$ was applied to the speed controller, while the motor has been loaded by $T_L = 90 N.m.$ at $t = 0.1\text{sec}$. The simulation results are presented in figures(13), (14) and (15).

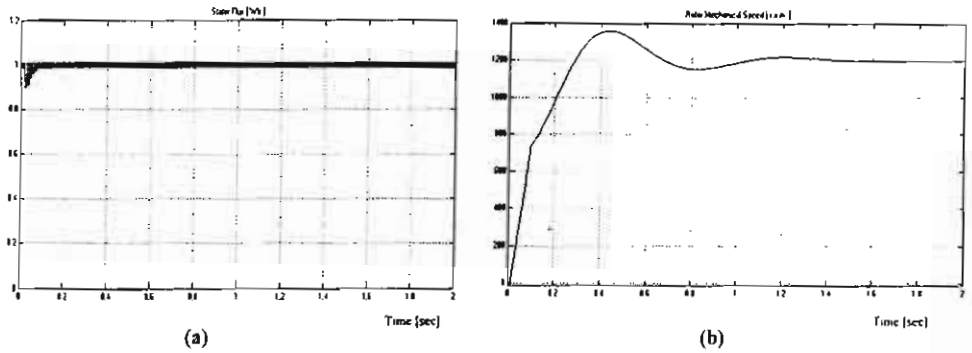

(a) (b)

Figure (13) (a) Stator flux (λ_s) (b) Motor speed (N_r)

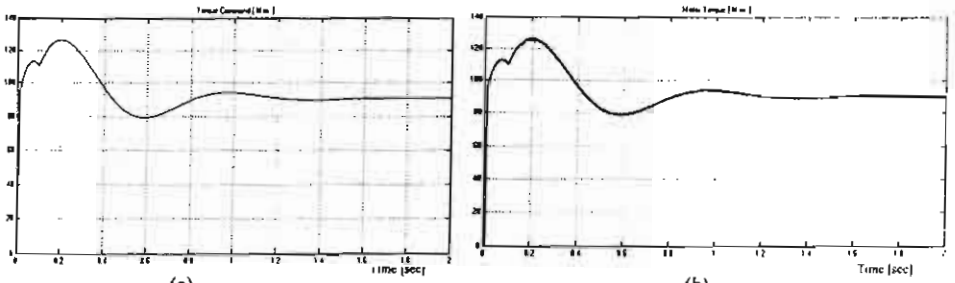

(a) (b)

Figure (14) (a) Torque command signal (T_e^*) (b) Motor torque (T_e)

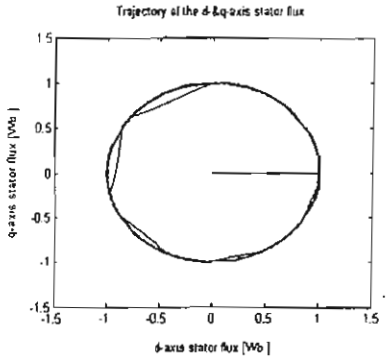

Figure (15) Stator flux space phasor during simulation

Figure (16) shows the electromagnetic torque response of the machine at starting.

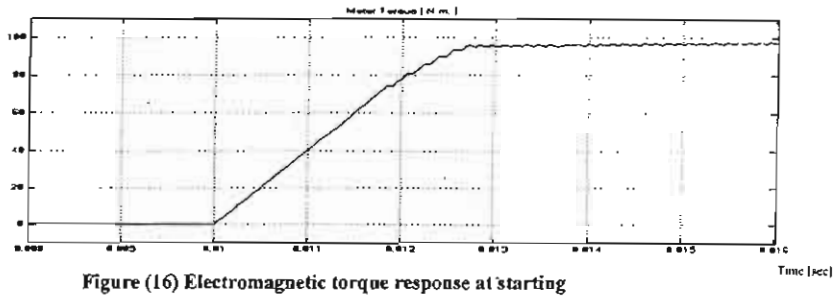

Figure (16) Electromagnetic torque response at starting

V. Fuzzy logic Direct Torque Control

The proposed fuzzy logic controller was designed to have three fuzzy state variables and one control variable for achieving constant torque and flux control. The first variable "ε_λ", which is the stator flux error signal, defined as:

$$\varepsilon_\lambda = \lambda_{sref} - \lambda_s \quad (4)$$

The second variable "ε_T", which is the motor torque error signal, defined as:

$$\varepsilon_T = T_{eref} - T_e \quad (5)$$

The third fuzzy state variable is the stator flux vector position (θ_s), defined as:

$$\theta_s = \tan^{-1}\left(\frac{\lambda_{qs}}{\lambda_{ds}}\right) \quad (6)$$

Then, the three input variables are divided into their fuzzy segments, where the number of fuzzy segments is chosen to have maximum control with a minimum number of rules. The universe of discourse of the stator flux error is divided into three linguistic variables with triangular and trapezoidal membership functions, where N, Z, and P denotes for negative, zero, and positive value of stator flux error, respectively, as shown in figure (17-a). The universe of discourse of the motor torque error is divided into five linguistic variables with triangular and trapezoidal membership functions, where NL, NS, Z, PS, and PL denotes for negative large, negative small, Zero, positive small, and positive large value of motor torque error, respectively, as shown in figure (17-b).

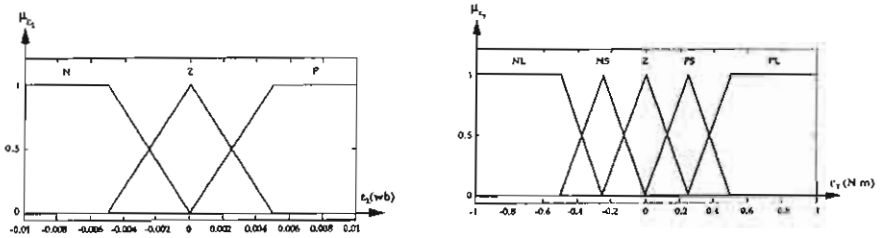

(a) (b)

Figure (17) (a) Membership functions for flux error signal
(b) Membership functions for torque error signal

For more accuracy, the universe of discourse of the stator flux vector position (θ_s) is divided into twelve fuzzy sets denoted (θ_1) to (θ_{12}), as shown in figure (18).

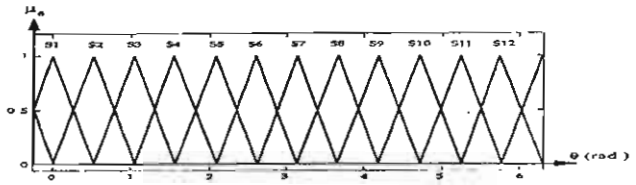

Figure (18) Membership function for stator flux position

The control variable is the inverter switching state (n). In a six-step inverter, seven distinct switching states are possible. Therefore, the universe of discourse of the controller output is divided into seven fuzzy sets, with triangular membership functions as shown in figure(19).

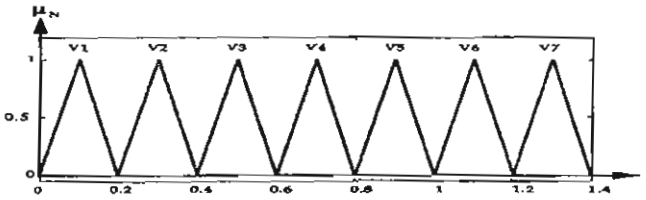

Figure (19) Membership functions for control output

The computation of stator flux position (θ_s) can be achieved using a digital circuit, which has been designed using MATLAB/SIMULINK, as shown in figure (20):

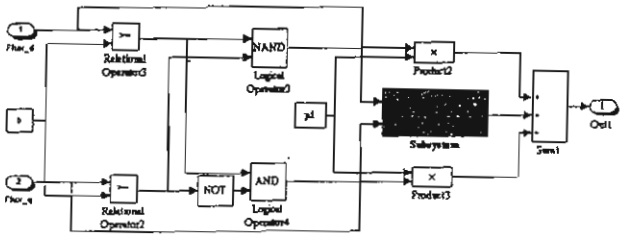

Figure (20) MATLAB/SIMULINK block diagram used to compute the stator flux position vector.

To achieved an accurate control action, the controller has been designed using Mamdani's inference method [11], based on min-max decision. The membership functions of variables A, B, C and N are given by μ_A, μ_B, μ_C and μ_N respectively. The weighting factor (α_i) for i^{th} rule can be written as:

$$\alpha_i = \min(\mu_{Ai}(\varepsilon_\lambda), \mu_{Bi}(\varepsilon_T), \mu_{Ci}(\theta_s)) \quad (7)$$

As mentioned before, the interface method was developed using Mamdani's minimum operation rule according to which the i^{th} rule leads to the control decision:

$$\mu'_{Ni}(n) = \min(\alpha_i, \mu_{Ni}(n)) \quad (8)$$

Thus, the membership function (μ_N) of the output (n) (i.e. the N^{th} rule) is point wise given by:

$$\mu_N(n) = \max_{i=1}^{180} (\mu'_{Ni}(n)) \quad (9)$$

In this case, the outputs are crisp; the Mean-Max method is used for defuzzification. By this method, the value of fuzzy output need to be digitalized using binary-to-decimal coded converter and some of logical and relational operators, as shown in figure(21), to generate three digital logic signals, that select the proper switching states of the inverter.

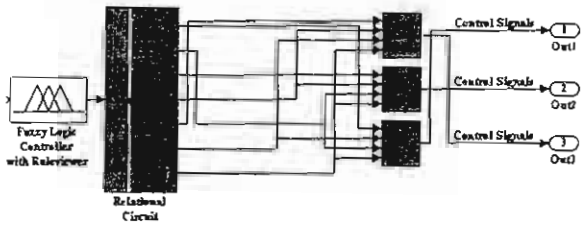

Figure (21) MATLAB/SIMULINK block diagram used to convert the crisp fuzzy output to three digital signals

The rules are formulated according to the effect of each discrete voltage vector on stator flux space vector that passes over the twelve sectors, as shown in figure (22).

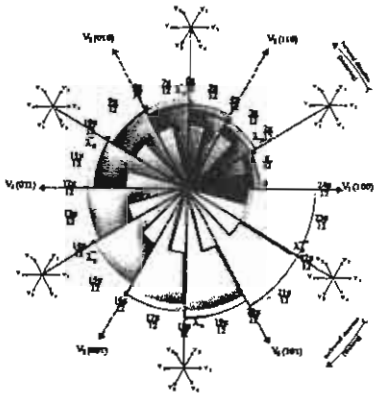

Figure (22) Selection of optimum voltage vectors as the stator flux space phasor passes over the twelve sectors

There are totally 180 rules [12], which are derived from the above figure, as shown in table (3) in the appendix.

VI. Simulation Results of Fuzzy DTC

A fuzzy controller that implements the direct torque control of an induction motor has been designed and simulated using FUZZY toolbox and SIMULINK under Matlab Ver.6 software package. Figure (23) shows the simulation block diagram of the fuzzy logic controller for a direct torque control of an induction motor.

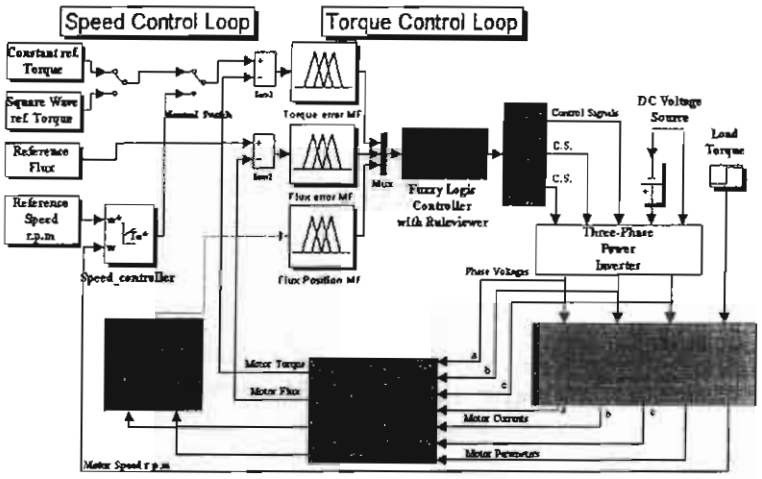

Figure (23) MATLAB/SIMULINK block diagram

1. Simulation of a Fuzzy Logic DTC with a Step-Input Reference Torque

The system was initially commanded by the rated stator flux as a constant reference value $|\lambda_s|^* = 1Wb.$ at $t = 0\sec.$, while the reference torque command signal was zero ($T_e^* = 0N.m.$). At $t = 0.01\sec.$, a step change from zero to the rated motor torque $T_e^* = 100N.m.$ was applied as a constant torque command signal, while the motor has been loaded by $T_L = 90N.m.$ at $t = 0.1\sec$. The simulation results are presented in figure(24), (25) and (26).

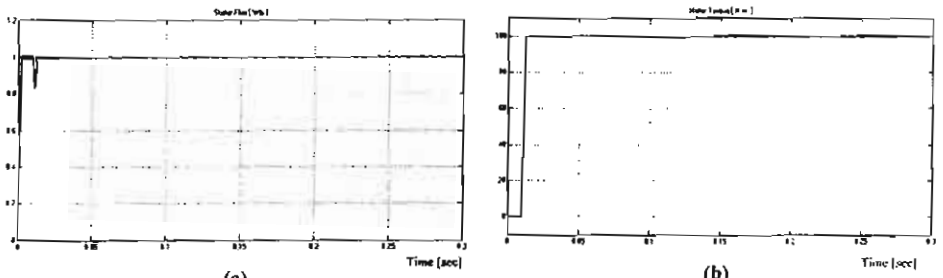

(a) (b)

Figure (24) (a) Stator flux response (λ_s) (b) Motor torque response (T_e)

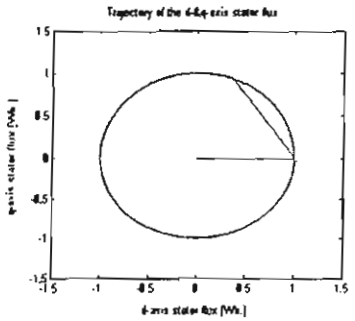

Figure (25) Stator flux space phasor during simulation.

Figure (26) shows the stator flux response and motor torque response of the machine at starting.

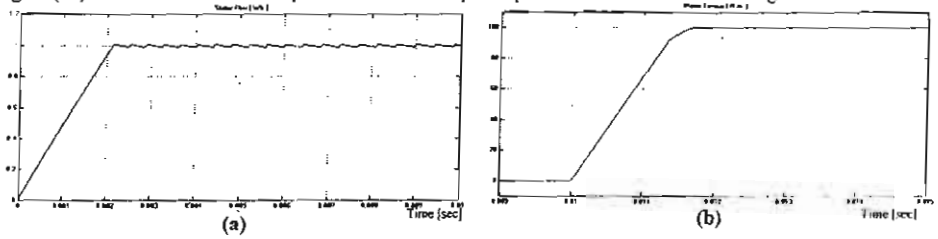

(a) (b)

Figure (26) (a) Stator flux response at starting (b) Motor torque response at starting

2. Simulation of a Fuzzy Logic DTC with a Square Wave Reference Torque

At $t = 0.01$sec. up to $t = 0.1$sec., a step change from zero to the rated motor torque $T_e^* = 100N.m.$ was applied as a constant torque command signal. At $t = 0.1$sec. a step change in torque command signal was applied to force it to be zero $T_e^* = 0N.m.$, and this sequence is repeated along the simulation. The simulation results are presented in figure(27), (28) and (29).

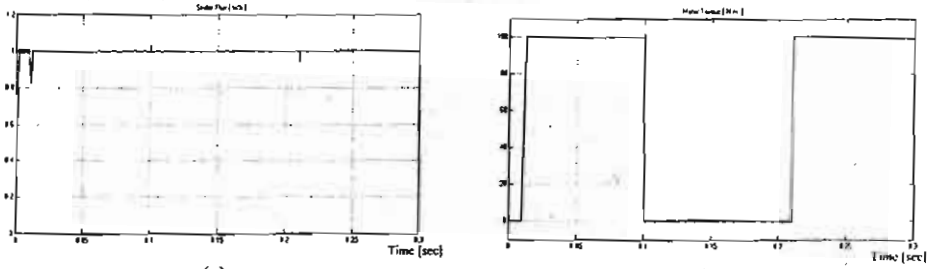

(a) (b)

Figure (27) (a) Stator flux (λ_s). (b) Motor torque (T_e).

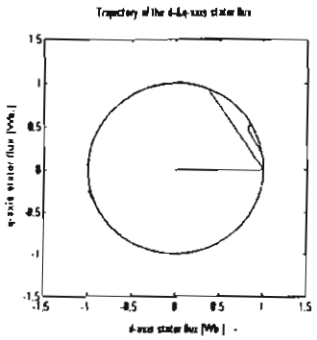

Figure (28) Stator flux space phasor during simulation

Figure (29) shows the electromagnetic torque response for a step change in torque command signal (step down).

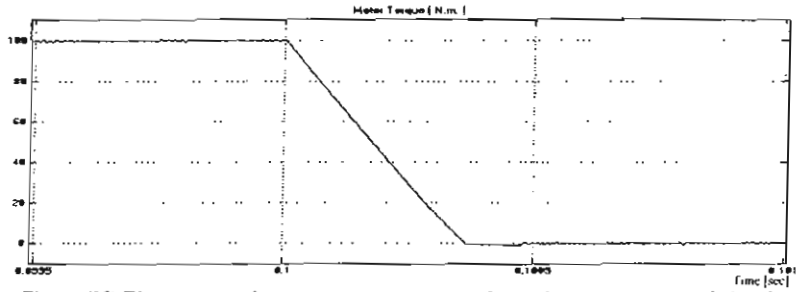

Figure (29) Electromagnetic torque response at step change in torque command signal.

3. Simulation of a Fuzzy Logic DTC with Speed Feedback Loop Using PI Controller

The system was initially commanded by the rated stator flux as a constant reference value $|\lambda_s|^* = 1Wb.$ at $t = 0\sec$, while the reference command of the speed controller was zero ($N_r^* = 0r.p.m.$). At $t = 0.01\sec.$, a step change from zero speed to motor rated speed $N_r^* = 1200r.p.m.$ was applied to the speed controller, while the motor has been loaded by $T_L = 90N.m.$ at $t = 0.1\sec$. The simulation results are presented in figure(30), (31) and (32).

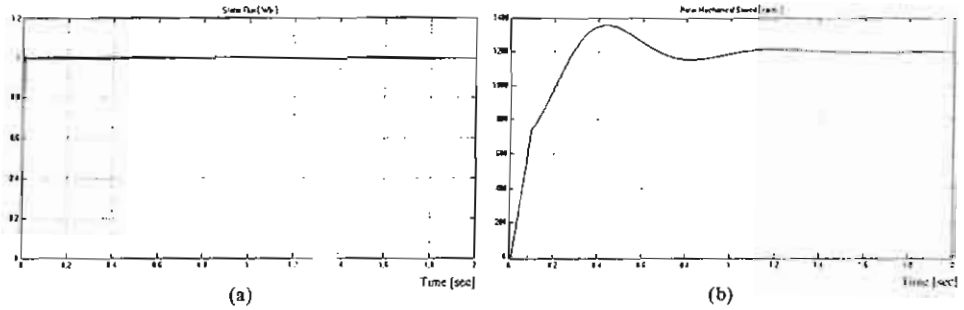

(a) (b)

Figure (30) (a) Stator flux (λ_s) (b) Motor speed (N_r)

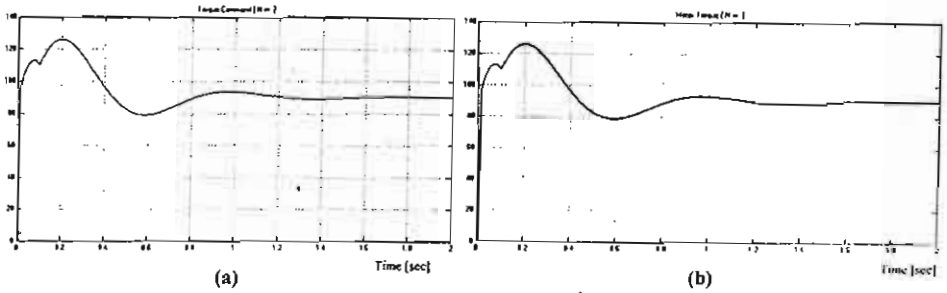

(a) (b)

Figure (31) (a) Torque command signal (T_e^*) (b) Motor torque (T_e)

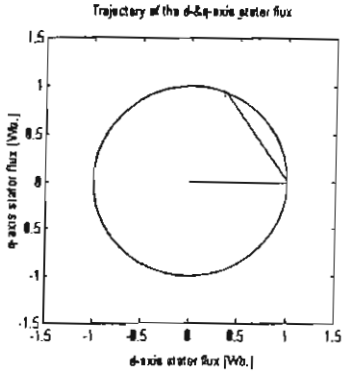

Figure (32) Stator flux space phasor during simulation

VII. Conclusions

The aim of this paper is based on the simulation of DTC of an I.M. using both of the conventional DTC and a new proposed technique for DTC based on fuzzy logic concept (F.DTC). The conventional DTC and F.DTC. Both of them were designed using MATLAB/SIMULINK software package. Also, MATLAB/FUZZY/INFERENCE SYSTEM (FIS) software was used to implement the fuzzy controller. Both were simulated under the same conditions. The differences between them have been investigated through a computer simulator. As a conclusion from the comparative study, the comparison was focused on the following items:

- fuzzy logic control F.DTC can differentiate between a small and relatively large error of torque and/or flux. Subsequently, the switching state selection would be more accurate to achieve the system requirements.
- In conventional DTC, the flux space was divided into six sectors, while in fuzzy logic control it is divided to twelve sectors to avoid the borderline effect of some states during the switching states selection.
- Using fuzzy logic control, the torque response records an approximate settling time of 1.7 millisecond for step-up command signal, and 0.35 millisecond for step-down. while, using conventional DTC, the torque response records an approximate settling time of 3 millisecond for step-up command signal, and 0.6 millisecond for step-down.
- Using fuzzy logic control provides the system with minimum ripple for both torque and flux. where the peak-to-peak flux ripple is $\pm 0.004 Wb.$, and the peak-to-peak torque ripple is $\pm 0.3 N.m.$ While the conventional DTC have a relatively large ripple, where the peak-to-peak flux ripple was $\pm 0.01 Wb.$, and the peak-to-peak torque ripple was $\pm 1 N.m.$

Finally, the simulation results show an improvement with fuzzy controller over the conventional DTC in both flux and torque responsesl. The steady state response for both controllers was found to be relatively the same.

VIII. Appendix

Table (2) Parameters of the selected Induction Motor

No.	Definition	Symbols	Data/Unit
1	Rated output	P_N	18.5 KW
2	Rated Voltage	V_N	460 Volt
3	Rated Frequency	f_N	50 Hz
4	Rated Speed	n_N	1465 r/min
5	Rated Current	I_N	34.4 Amp.
6	Nominal Torque	T_N	121 N.m.
7	Power Factor		0.85
8	Moment of inertia	J	0.161 Kg-m^2
9	Viscous Coefficient	B	0.0018635 N.m./rad/sec
10	Stator Resistance	R_s	0.2 Ohm
11	Rotor Resistance	R_r	0.15 Ohm
12	S-Self Reactance	X_s	0.41 Ohm
13	R-Self Reactance	X_r	1.42 Ohm
14	Magnetizing React.	X_m	18.8 Ohm
15	Number of Poles	P_n	4 Pole

Table (3) Lookup table of fuzzy rules for voltage vector selection

e_T \ e_λ	$e_{\lambda p}$	$e_{\lambda z}$	$e_{\lambda n}$
e_{Tp}	1	2	2
e_{Tz}	1	2	3
e_{Tn}	7	7	7
e_{Tnn}	6	7	4
e_{Tnn}	6	5	5

S1

e_T \ e_λ	$e_{\lambda p}$	$e_{\lambda z}$	$e_{\lambda n}$
e_{Tp}	2	2	3
e_{Tz}	2	3	3
e_{Tn}	7	7	7
e_{Tnn}	6	7	5
e_{Tnn}	6	6	5

S2

e_T \ e_λ	$e_{\lambda p}$	$e_{\lambda z}$	$e_{\lambda n}$
e_{Tp}	2	3	3
e_{Tz}	2	3	4
e_{Tn}	7	7	7
e_{Tnn}	1	7	5
e_{Tnn}	1	6	6

S3

e_T \ e_λ	$e_{\lambda p}$	$e_{\lambda z}$	$e_{\lambda n}$
e_{Tp}	3	3	4
e_{Tz}	3	4	4
e_{Tn}	7	7	7
e_{Tnn}	1	7	6
e_{Tnn}	1	1	6

S4

e_T \ e_λ	$e_{\lambda p}$	$e_{\lambda z}$	$e_{\lambda n}$
e_{Tp}	3	4	4
e_{Tz}	3	4	5
e_{Tn}	7	7	7
e_{Tnn}	2	7	6
e_{Tnn}	2	1	1

S5

e_T \ e_λ	$e_{\lambda p}$	$e_{\lambda z}$	$e_{\lambda n}$
e_{Tp}	4	4	5
e_{Tz}	4	3	5
e_{Tn}	7	7	7
e_{Tnn}	2	7	1
e_{Tnn}	2	2	1

S6

e_T \ e_λ	$e_{\lambda p}$	$e_{\lambda z}$	$e_{\lambda n}$
e_{Tp}	4	5	5
e_{Tz}	4	5	6
e_{Tn}	7	7	7
e_{Tnn}	3	7	1
e_{Tnn}	3	2	2

S7

e_T \ e_λ	$e_{\lambda p}$	$e_{\lambda z}$	$e_{\lambda n}$
e_{Tp}	5	5	6
e_{Tz}	5	6	6
e_{Tn}	7	7	7
e_{Tnn}	3	7	2
e_{Tnn}	3	3	2

S8

e_T \ e_λ	$e_{\lambda p}$	$e_{\lambda z}$	$e_{\lambda n}$
e_{Tp}	5	6	6
e_{Tz}	5	6	1
e_{Tn}	7	7	7
e_{Tnn}	4	7	2
e_{Tnn}	4	3	3

S9

e_T \ e_λ	$e_{\lambda p}$	$e_{\lambda z}$	$e_{\lambda n}$
e_{Tp}	6	6	1
e_{Tz}	6	1	1
e_{Tn}	7	7	7
e_{Tnn}	4	7	3
e_{Tnn}	4	4	3

S10

e_T \ e_λ	$e_{\lambda p}$	$e_{\lambda z}$	$e_{\lambda n}$
e_{Tp}	6	1	1
e_{Tz}	6	1	2
e_{Tn}	7	7	7
e_{Tnn}	5	7	3
e_{Tnn}	5	4	4

S11

e_T \ e_λ	$e_{\lambda p}$	$e_{\lambda z}$	$e_{\lambda n}$
e_{Tp}	1	1	2
e_{Tz}	1	2	2
e_{Tn}	7	7	7
e_{Tnn}	5	7	4
e_{Tnn}	5	5	4

S12

IX. References

[1] Ion Boldea and Syed A. Nasar, "Vector Control of AC Drives", CRC Press, Boca Raton, Florida, 1992. (Book)

[2] Domenico Casadei, Giovanni Serra. and Angelo Tani, "Implementation of a Direct Torque Control Algorithm for I M Based on Discrete Space Vector Modulation", IEEE Trans. on Power Electronics, Vol. 15, No. 4, July 2000.

[3] Hoang Le-Huy, "Behavior Modeling and Simulation of a Direct-Torque-Control Induction Motor Drive Using PSPICE". Department of Electrical and Computer Engineering, University Laval, Ste-Foy, Quebec, Canada, 2000.

[4] M. E. Nillesen, J. L. Duarte, M. Pasquariello, and A. Del Pizzo, "Direct Torque Control with the Application of a Predictive Pulse Width Control", Eindhoven University of Technology, Universita Napoli "Federicoll". Netherlands, Napoli, Italy, 2000.

[5] Anthony Purcell and Paul P. Acarnley, "Enhanced Inverter Switching for Fast Response Direct Torque Control". IEEE Trans. on Power Electronics, Vol. 16, No 3, May 2001.

[6] Uwe Baader, Manfred Depenbrock, and Georg Gierse, "Direct Self Control (DSC) of Inverter-Fed Induction Machine: A Basic for Speed Control without Speed Measuring", IEEE Trans. on Ind. Appl., Vol. 28, No. 3, pp 581-588. May/June 1992.

[7] L. A. Zadah, "Fuzzy Sets", Information and Control, Vol. 8, pp. 338-353, 1965

[8] Leonid Reznik, "Fuzzy Controllers", Oxford, Boston, Johann, N. D, Sing, Linacre House, Jordan-Hill. 1997 (Book)

[9] A. A. Khalil, "Micro-Computer Based Fuzzy Logic Protection of AC Drive", Ph. D, Ain Shams University. 1999.

[10] L. H. Tsoukvlas and R. E. Uhrig, "Fuzzy and Neural Approaches in Engineering", Jhon Wiley and Sons, inc., 1997. (Book)

[11] D. Dubois and H. Parade, "Fuzzy Sets and Systems: Theory and Applications", Academic Press. Boston. 1980. (Bonk)

[12] T. Terano, K. Asai, and M. Sugeno, "Fuzzy System Theory and its Applications", Academec Press. Boston, 1992.

[13] B. Kosko, "Fuzzy Thinking: The New Science of Fuzzy Logic", Harper Collins, G. B., 1994. (Book)

[14] M. Jamshidi, N. Vadiee, and T. Ross, "Fuzzy Logic and Control: Software and Hardware Applications", Prentice-Hall, Englewood Cliffs, N. J., 1993.

[15] ISAO Takahashi and Toshihiko Noguchi, "A New Quick Response and High Efficiency Control Strategy of an I M". IEEE IAS Ann. Mtg., pp. 496-502, 1985.

[16] MATLAB, "Full Product Family Help FIS", Matlab Manual Version 6.0 0 88, Release 12, MathWork Inc. September 22, 2000. (Book)